

Observational evidences of Walker circulation change over the last 30 years contrasting with GCM results

B. J. Sohn · Sang-Wook Yeh · Johannes Schmetz · Hwan-Jin Song

Received: 13 January 2012 / Accepted: 2 August 2012 / Published online: 14 August 2012
© The Author(s) 2012. This article is published with open access at Springerlink.com

Abstract In order to examine the changes in Walker circulation over the recent decades, we analyzed the sea surface temperature (SST), deep convective activities, upper tropospheric moistening, sea level pressure (SLP), and effective wind in the boundary layer over the 30-year period of 1979–2008. The analysis showed that the eastern tropical Pacific has undergone cooling while the western Pacific has undergone warming over the past three decades, causing an increase in the east–west SST gradient. It is indicated that the tropical atmosphere should have responded to these SST changes; increased deep convective activities and associated upper tropospheric moistening over the western Pacific ascending region, increased SLP over the eastern Pacific descending region in contrast to decreased SLP over the western Pacific ascending region, and enhanced easterly wind in the boundary layer in response to the SLP change. These variations, recognized from different data sets, occur in tandem with each other, strongly supporting the intensified Walker circulation over the tropical Pacific Ocean. Since the SST trend was attributed to more frequent occurrences of central Pacific-type El Niño in recent decades, it is suggested that the decadal variation of El Niño caused the intensified

Walker circulation over the past 30 years. An analysis of current climate models shows that model results deviate greatly from the observed intensified Walker circulation. The uncertainties in the current climate models may be due to the natural variability dominating the forced signal over the tropical Pacific during the last three decades in the twentieth century climate scenario runs by CMIP3 CGCMs.

Keywords Walker circulation · El Niño · Decadal variation · Climate change over the tropics

1 Introduction

Global warming caused by an increased emission of anthropogenic greenhouse gases has been occurring since the industrial revolution (IPCC 2007), and the sea surface temperature (SST) and heat content of tropical oceans have increased significantly in recent decades (e.g., O’Carroll et al. 2006; Levitus et al. 2009). Consequently, the geographical redistribution of diabatic heating can be expected in response to the associated SST changes, causing circulation changes in the atmosphere. Furthermore, there is evidence that a long-term trend showing weakened Walker circulation over the course of the twentieth century in both climate models and observations of sea level pressure (SLP) (Vecchi and Soden 2007), consistent with the expectation that the circulation will be weakened because of thermodynamic and hydrological constraints under the warmed Earth–atmosphere system (Held and Soden 2006).

However, even if the slowdown of the circulation is accepted as a long-term trend through both the twentieth and the twenty-first centuries, we cannot rule out the possibility that the hydrological constraints or slowdown of the

B. J. Sohn (✉) · H.-J. Song
School of Earth and Environmental Sciences, Seoul National University, NS80, Seoul 151-747, Korea
e-mail: sohn@snu.ac.kr

S.-W. Yeh
Department of Environmental Marine Science,
Hanyang University, Ansan, Korea

J. Schmetz
EUMETSAT, Darmstadt, Germany

circulation may not occur locally or during short-term climate changes. In fact, it has been shown that east–west SST gradients over the tropical Pacific Ocean basin can be increased through the contributions of ocean dynamics (Clement et al. 1996; Sun and Liu 1996; Cane et al. 1997; Seager and Murtugudde 1997; Karnauskas et al. 2009) rather than the more homogenous SST increases often shown in GCM simulations (e.g. Vecchi et al. 2008). Therefore, enhanced east–west Walker circulation may be expected despite global warming, in response to the SST changes over the tropics.

In fact, satellite observations and reanalysis have indicated the strengthening of the Walker circulation (Sohn and Park 2010; Meng et al. 2011; Zahn and Allan 2011; Zhou et al. 2011). In particular, microwave-based Special Sensor Microwave Imager (SSM/I) measurements of the water budget parameters indicated that the Walker circulation has intensified over the 18-year observation period from 1988 to 2005 (Sohn and Park 2010). In this study, we seek further observational evidence supporting the strengthening of the Walker circulation over the recent three decades. In the mean climatological Walker circulation over the tropical Pacific, a broad ascending branch resides over the western Pacific–Indian Ocean warm pool region, which is connected to a descending branch over the eastern Pacific cold waters. If Walker circulation is enhanced, deep convective activities should enhance over the western Pacific ascending region. Because deep convective clouds are the main contributors to the moistening of the upper troposphere over tropical convective regions (e.g., Sohn et al. 2008; Chung et al. 2009), increased upper tropospheric humidity (UTH) can be expected in accordance with the increased convection over the western Pacific. The eastern Pacific descending branch, on the other hand, may get increasingly dry. Because of the mass overturning caused by the intensified upward motion over the ascending branch, the eastern Pacific descending region should experience increased SLP, establishing a stronger east–west SLP gradient in conjunction with the decreased SLP over the western Pacific ascending region. As a consequence, in the lower branch of the Walker cell, easterly trade wind should increase.

In this study, we examine the long-term variations in the atmospheric variables that might be sensitive to changes in the Walker circulation; we use satellite and surface observations to examine whether these observations agree with a working hypothesis of intensified Walker circulation. We further examine the decadal SST variations over the tropics as a possible cause of the intensified Walker circulation. The results should be relevant to our current level of understanding of the global climate change simulations by climate models.

2 Datasets and analysis methods

The SST dataset used in this study is the Hadley Centre Sea Ice and Sea Surface Temperature (HadISST; Rayner et al. 2003) given in a $1^\circ \times 1^\circ$ grid format (downloaded from <http://hadobs.metoffice.com/hadisst/data/download.html>). Monthly mean values are available from 1850 onward, and in this study, data from the last 30 years (1979–2008) are used. It is worthwhile to note that we also analyzed the extended reconstructed SST version 3 (ERSST v3, Smith et al. 2008) in the same period (i.e., 1979–2008) and found few results changed in spite of the use of different SST datasets. It is because our main interest lies in the last three decades from late 1970s. There exist some differences in terms of their linear trends in the tropical Pacific among multiple SST datasets (Deser et al. 2010; L’Heureux et al. 2012); however, such discrepancies are usually raised when a long-term period of SST dataset is considered (e.g., Park et al. 2012). Thus, in this paper, all results are presented based on the HadISST data set.

Examining temporal and spatial variation in deep convective activities over the tropics, we use the frequency of occurrence of deep convective cloud obtained from the weather state (WS) analysis of the International Satellite Cloud Climatology Project (ISCCP) cloud data (Jakob and Tselioudis 2003; Rossow et al. 2005). Various WS-related cloud regimes (e.g., deep convective cloud, anvil, and cirrus) were defined by applying the K-means clustering method to cloud top pressure (CTP)–cloud optical thickness (COT) histograms. It has been suggested that the WS analysis largely reflects the cloud morphology and is less sensitive to the satellite calibration or sampling method and is thus more appropriate for examining the long-term trend of convective activities (Tselioudis et al. 2010). Daily occurrences of deep convective weather state (downloaded from <http://isccp.giss.nasa.gov/etcluster.html>) are counted at each grid point, and monthly frequencies are obtained by cumulating the daily frequencies over the tropical and subtropical regions (35°N – 35°S) over the 25 years from July 1983 to June 2008.

It is well known that deep convection is mainly responsible for moistening the upper troposphere over the tropics (Sohn et al. 2008). However, the moistening mechanism over the descending region is rather complicated because of lateral mixing with high-latitude air (Roca et al. 2012). In order to relate changes in the UTH to convective activities over the warm pool region, we use three-decade-long NOAA HIRS channel brightness temperature (TB) around the $6.7\text{-}\mu\text{m}$ water vapor absorption band (Shi and Bates 2011), in which the channel’s weighting function is around the 200–500 hPa layer. Instead of converting the TB into relative humidity, only

the TB trend is examined, as its variations are predominantly modulated by the UTH changes (Table 1 of Soden and Bretherton 1993). Positive (negative) TB anomalies from the mean condition represent drier (wetter) conditions than normal. The monthly mean TBs of the HIRS water vapor channel span 30 years (1979–2008) in the 2.5° grid format and were downloaded from <ftp://eclipse.ncdc.noaa.gov/pub/hirs/hirsch12monthlygrid>.

The monthly mean SLP data from the Hadley Centre data version 2 (HadSLP2; Allan and Ansell 2006; available from <http://www.hadobs.metoffice.com/hadslp2>) are used to examine changes in the SLP gradient between the centers of the Walker circulation branches in the eastern Pacific and western Pacific. From the collection of SLP data, only 30-year (1979–2008) data given in $2^\circ \times 2^\circ$ grid format are used.

To examine whether surface wind variation is coherent with the hypothesized increased Walker circulation or other variables, the effective boundary-layer wind field is obtained from water vapor transport scaled by the total column water vapor (i.e., $V_E = Q/TPW$, where Q is the column-integrated water vapor flux). It is because the water vapor is mainly transported through the lower returning branch of the Walker circulation cell, and thus the effective wind can be represented as the circulation intensity. On the other hand, averaged boundary layer wind is difficult to use as an index because of the varying boundary layer depth across the Pacific Ocean basin. Detailed discussion on the effective boundary-layer wind (V_E) is found in Sohn and Park (2010). It has been noted that the reanalysis results are very similar to those suggested by the SSM/I measurements. Because the SSM/I observations are only available from 1988 to 2005, we use ERA-Interim reanalysis data (Simmons et al. 2006) for computing water vapor flux and then V_E , based on the assumption that the trend analysis results would not be discernible from satellite observations. In fact, it is noted that the trend of the east–west component of the effective wind of ERA-Interim reanalysis, averaged over the tropical Pacific (150°E – 165°W , 15°N – 7.5°N), appears to be slightly smaller than an SSM/I-suggested value (i.e., -0.046 ms^{-1} vs. -0.062 ms^{-1} per 10 years). ERA-Interim reanalysis data provide moisture and wind information at 37 levels from 1,000 to 1 hPa; however, only the lowest 23 levels from 1,000 to 200 hPa are used for the column-integrated water vapor flux calculation.

3 Results

In order to examine the spatially coherent patterns of temporal variations in climate variables that are considered to be facets of the Walker circulation changes, the Empirical Orthogonal Function (EOF) analysis is conducted for the

SST, deep convection (DC), HIRS $6.7\text{-}\mu\text{m}$ water vapor channel TB (hereafter referred to as TB_{WV}), SLP, and water vapor transport (WVP) effective wind (V_E). The EOF analysis is considered to be an effective way of analyzing temporally varying spatial patterns for any field of interest over a specified area. A trend analysis of the principal component (PC) time series is also conducted, and the obtained linear trend is considered for discussion if the t test satisfies the 99 % confidence level ($t > 2.58$ for 360 months). Results are displayed in Fig. 1.

The first EOF mode of the SST, contributing 40.4 % of the total variance over 30 years (1979–2008) over the tropical Indian and Pacific Oceans, depicts the well-known El Niño/La Niña pattern (Fig. 1a). Note that the negative anomalies situated over the central and eastern tropical Pacific are largely comparable to the change of tropical Pacific mean state (shown later in Fig. 3). By combining the vector loadings with the associated PC time series, one can find distinct positive SST anomalies over the equatorial eastern Pacific and horseshoe-like cold anomalies surrounding the warm anomaly regions during El Niño years such as 1982–1983, 1987–1988, and 1997–1998. Less salient but positive anomalies are also clearly visible during other El Niño years (1986–1987, 1991–1992, 1994–1995, 2002–2003, 2004–2005, 2006–2007). During La Niña years, very low SST anomalies over the eastern Pacific and high SST anomalies over the western Pacific are noted.

The PC time series on the right panel shows that there exists a significant positive trend. Recently, McPhaden et al. (2011) and Feng et al. (2010) argued that there have been systematic changes in the background conditions over the last three decades, i.e., 1980–2010. They also showed that the SSTs were slightly cooler in the eastern Pacific and warmer in the western Pacific during the first decade of the twenty-first century than during the last two decades of the twentieth century; this result is consistent with the positive trend shown in the first EOF PC time series (Fig. 1a).

The first EOF mode of DC anomalies, explaining approximately 10.2 % of the total DC variance, shows a dipole-like pattern over the tropical Pacific (Fig. 1b), where a positive anomaly area is situated over the Maritime Continent in contrast to the negative anomaly area over the central Pacific between 150°E and 150°W . Dominant positive loadings are also evident in the South Pacific Convergence Zone (SPCZ) extending from east New Guinea to the South Pacific over the 30°S – 150°W region. It should be noted that the time series shows a striking similarity to that for SST PC1, including the positive linear trend. Thus, over the tropical Pacific Ocean, deep convective activities appear to be closely associated with El Niño and La Niña events. For example, during the 1997–1998 El Niño, deep convective activities were

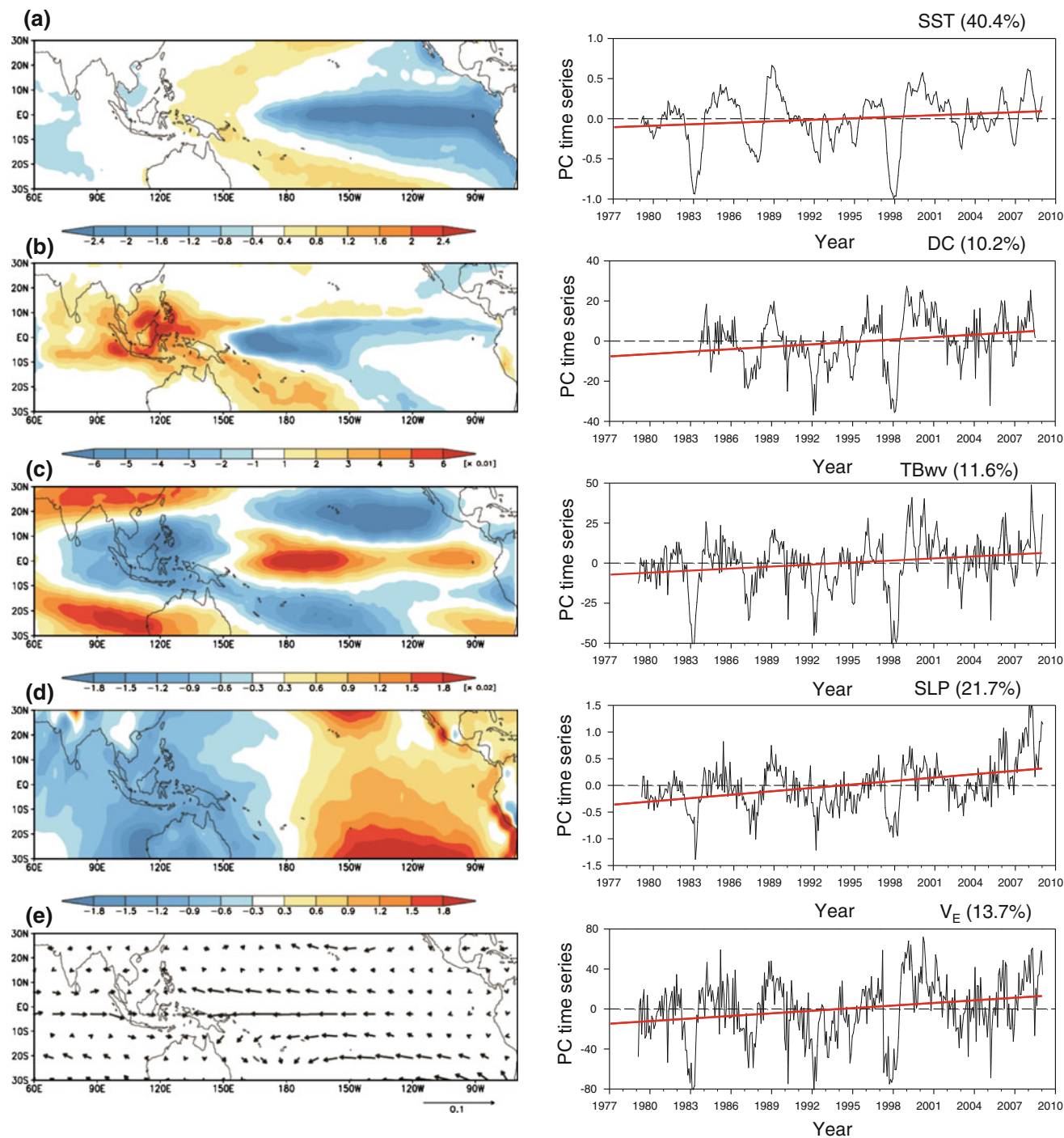


Fig. 1 First leading eigenvector and time series of the associated principal component obtained from the EOF analysis of **a** SST, **b** DC, **c** TBwv, **d** SLP, and **e** V_E . Monthly anomalies are computed by

removing the mean seasonal cycle based on the 30 year climatology, except DC, which is based on a 25-year mean

greatly suppressed over the western Pacific while considerably enhanced deep convective activities were found over the central Pacific. Furthermore, the long-term trend of the PC time series of the EOF mode 1 of DC (Fig. 1b) indicates that convective activities over the Indo-Pacific

warm pool have been enhanced for the last three decades, in contrast to reduced activities over the central and eastern tropical Pacific, which is largely consistent with a positive trend in the SSTs in the tropical Pacific basin, as shown in Fig. 1a.

The EOF mode 1 of TB_{WV} shows a near one-to-one correspondence to DC over equatorial areas (Fig. 1c), suggesting that variations in deep convective activities are the main cause of modulation of the UTH over the tropics. Considering that positive (negative) anomalies of TB_{WV} imply drier (wetter) than normal conditions, we find that the upper troposphere is much wetter during El Niño years over the central equatorial Pacific and much drier over the Indian Ocean. Again, the PC time series shows a near one-to-one correspondence to both the SST and the DC PC time series. The close resemblance of the PC time series between TB_{WV} and DC, and SST strongly suggests that DC anomalies in response to SST changes are directly responsible for the moisture variations in the upper troposphere over the convectively active region. Since the upper tropospheric moisture over the subtropics is significantly influenced by later mixing with the air mass in the higher latitudes (Roca et al. 2012), it is not surprising to find less correspondence over the subtropical dry regions in comparison to the strong correlation found over the equatorial region. Nevertheless, moisture variations over the subtropical oceans during the El Niño years appear to be largely controlled by the SST changes (and convection) there.

The EOF mode 1 of SLP, explaining 21.7 % of the total variance, shows an east–west separated pattern in the vector loading (Fig. 1d). The maximum negative loadings situated over the western tropical Pacific to the eastern Indian Ocean off west Australia are in contrast to the maximum positive loadings in the southeastern tropical Pacific, establishing a typical pattern of the Walker circulation. In gross aspect, it is very similar to the oscillating behavior of El Niño/Southern Oscillation (ENSO) when combined with the PC time series (Philander 1989). As expected from SST variations in conjunction with phase changes of ENSO, the PC time series of SLP mode 1 are remarkably coherent with that of SST.

Similar to the PC time series of the first EOF SST mode (Fig. 1a), it is evident that the PC time series of the first EOF SLP mode shows a significant positive linear trend (Fig. 1c). This clearly indicates that an east–west SLP difference (SLP in the east minus SLP in the west) has gradually increased during the last three decades, suggesting that the trade winds across the tropical Pacific basin became stronger. Not surprisingly, recent analysis of Pacific Ocean Sea surface height trends from satellite altimeter for the period of 1993–2009 also showed that dominant regional trends of increasing sea surface height over the western tropical Pacific have existed since the early 1990s relative to the preceding 40 years (Merrifield 2011). Such trends should indicate intensified easterly trade winds across the tropical Pacific.

The V_E EOF first mode, explaining approximately 13.7 % of the total variance, generally shows easterly

loadings over the tropical Pacific and westerly loadings over the tropical Indian Ocean, forming a convergence loading over the western Pacific warm pool region. Thus, when vector loadings are combined with negative PC values during strong El Niño years such as 1982–1983, 1997–1998, wind field anomalies in the boundary layer must be strong westerlies over the tropical Pacific Ocean basin, resulting in weaker easterlies (or reversed wind). The PC time series is remarkably similar to that found from four other variables, suggesting that all variables expressed by EOF mode 1 are consistent with each other in the context of strengthened Walker circulation over the last three decades.

It should be noted that the PC time series of DC, TB_{WV} , SLP, and V_E are all very similar to that of SST EOF mode 1; correlation coefficients between any pair of variables are listed in Table 1. Because the SST mode 1 represents a typical (or canonical) El Niño mode, the similar shapes of fluctuations discovered in DC, TB_{WV} , SLP, and V_E strongly suggest that their largest interannual variations are also related to ENSO. For example, during the 1997–1998 El Niño in which warm SSTs were prevalent in the equatorial Pacific, deep convective clouds were much suppressed in the western Pacific. Prevailing dryness over the western Pacific and Indian Ocean is clear when the positive TB_{WV} anomalies are taken into consideration, in response to suppressed deep convective clouds there. Overall, a shift of pressure pattern is obvious for the 1997–1998 El Niño period. Anomalous winds should be westerlies from the higher-pressure area over the western Pacific to the lower pressure area over the eastern Pacific, resulting in the well-known water vapor transport to the central Pacific (Sohn et al. 2004).

The close relationship of interannual variation in DC, TB_{WV} , SLP, and V_E first EOF mode to the ENSO variation is also evident in the regressed patterns against the NINO3 SST index, which is defined as the anomalous SST averaged in the NINO3 region (i.e.: 150°W–90°W, 5°N–5°S). As expected, it is noted that the spatial patterns of regressed parameters associated with ENSO are similar to those vector fields found in first EOFs (not shown here). The similarity implies that the first EOFs of different

Table 1 Correlation coefficient between paired EOF mode 1 time series

	DC	TB_{WV}	SLP	V_E
SST	0.82	0.80	0.70	0.74
DC		0.90	0.74	0.86
TB_{WV}			0.70	0.80
SLP				0.83

DC deep convective cloud, TB_{WV} HIRS 6.7 μm channel brightness temperature, SLP sea level pressure, V_E water vapor transport effective wind

parameters shown in Fig. 1 capture the variabilities in relation to ENSO.

Considering the SST PC time series correlation coefficients of 0.82, 0.80, 0.70, and 0.74 with DC, TB_{WV} , SLP, and V_E , respectively, we find that the SST changes cause coherent fluctuations amongst them. It is also clear that the UTH over the convective area is strongly controlled by deep convective activities. A highly correlative pattern is found between the SLP and the V_E PC time series, with a correlation coefficient of 0.83, suggesting that the effective wind deduced from water vapor transport must be closely tied to the surface pressure pattern.

More importantly, all PC time series show similar increasing trends at a 99 % confidence level. Recently, it has been reported that a new type of El Niño has emerged and has been given various names, e.g., date line El Niño (Larkin and Harrison 2005), El Niño Modoki (Ashok et al. 2007), central Pacific El Niño (Yeh et al. 2009; Kao and Yu 2009), and warm pool El Niño (Kug et al. 2009). This type of El Niño, referred to as central Pacific (CP) El Niño in this study, is characterized by anomalous warming in the central Pacific, in contrast to the conventional El Niño that shows the largest warming in the eastern Pacific and which is referred to as eastern Pacific (EP) El Niño in this study.

Increasing frequencies of CP El Niño are noted for the past three decades (for example, McPhaden et al. 2011). In order to examine the possible relations of the increasing trends found in the EOF mode 1 analysis to the El Niño variability, we also calculate intensities of El Niño and La Niña events following the approach of Lee and McPhaden (2010). Intensities are obtained within the central equatorial Pacific NINO4 region (160°E – 150°W , 5°N – 5°S) and within the eastern equatorial Pacific NINO3 region (150°W – 90°W , 5°N – 5°S) over the 30-year analysis period from 1979 to 2008 (Fig. 2). The ENSO variations shown in both indices indicate that the CP El Niño occurred more frequently than the EP El Niño in recent decades. In addition, the last decade of the analysis period (i.e. 1999–2008) is characterized by no strong EP El Niño such as 1982–1983 and 1997–1998 ones. By contrast there is no obvious trend of La Niña events in both frequency and intensity.

From above analysis, it is conjectured that the time series of SST mode 1 reflects fewer occurrences of conventional EP El Niño in the recent decade, in which their magnitude has become weaker. Conversely, the more frequent occurrence of CP El Niño, over the last 10 years (as shown in Fig. 2) appears to induce relatively cold

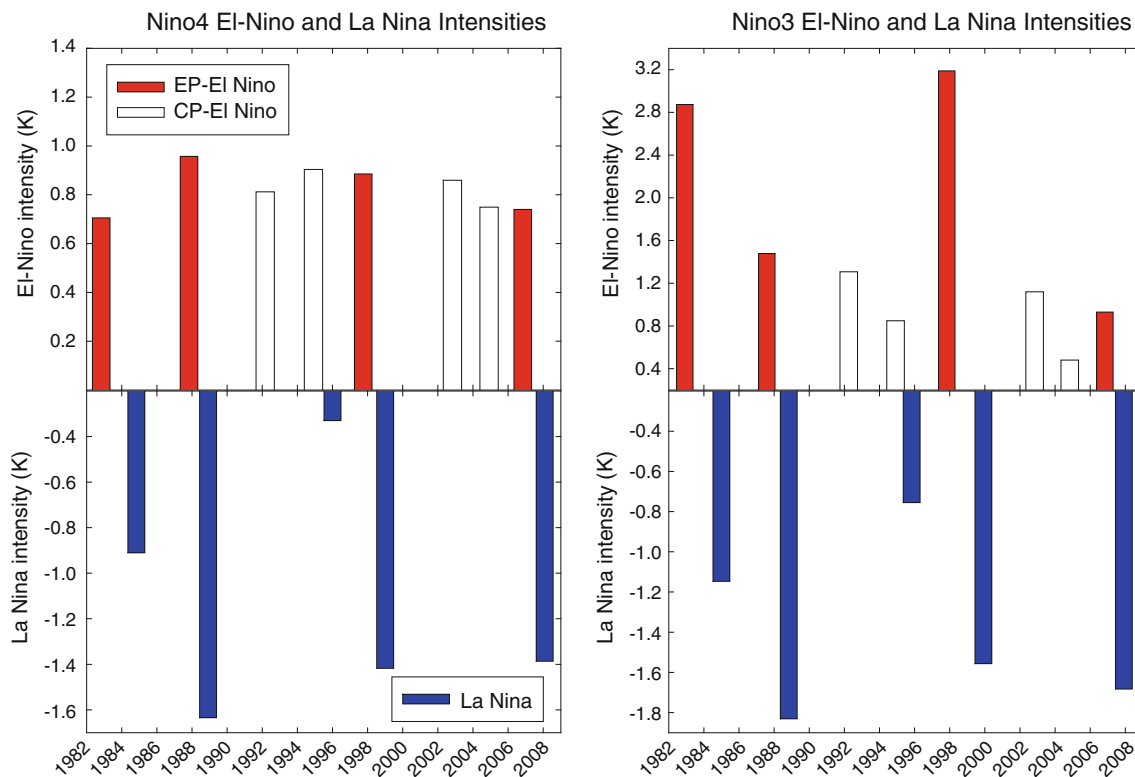


Fig. 2 Intensities of El Niño and La Niña events in the central equatorial Pacific (NINO4 region, *left panel*) and in the eastern equatorial Pacific (NINO3 region, *right panel*) over the 30 year analysis period (1979–2008). The intensities of El Niño and La Niña

events in the CP (EP) region are determined from the peak values of the three-month (December–January–February) smoothed Niño4 (Niño3) index

anomalies over the eastern Pacific and warm anomalies in the western Pacific. Indeed, fewer occurrences of EP El Niño and associated lower warming in the Pacific cold tongue in recent years appear to have caused the SST trend in the EOF mode 1, and other atmospheric variables should have followed the SST changes.

4 Impact of decadal variations in El Niño on the changes in the Walker circulation

We hypothesize that the more (less) frequent occurrence of CP (EP) El Niño in the last decade is the main cause of development of the distinct cooling SST trend and that other variables are coherent because of the response of the atmosphere to SST changes in the tropical Pacific. In order to examine this view, anomalies of five variables from the EOF mode 1 are constructed. Given the fact that the first decade of the twenty-first century is characterized by the predominant occurrence of CP El Niños (McPhaden et al. 2011), we take composite means for two periods, i.e., first 20 years (1979–1998) and last 10 years (1999–2008) over the last three decades.

To demonstrate the structural changes in five variables caused by El Niño variability over the last three decades, differences of the variability reconstructed by each first EOF mode in the two temporal periods (1999–2008 minus 1979–1998) are shown in right panels of Fig. 3. Also shown are the differences in mean fields over the same periods (left panels). It is done so because the EOF SST mode 1 represents the EP El Niño variability, and thus the mode 1 component difference is able to represent the mean SST difference due to the EP El Niño characteristics between the two periods, i.e., decreased EP El Niño frequency and weakened intensity from 1979–1998 to 1999–2008. We assume that if EP El Niño variability does not occur much between the two periods, there should be few meaningful patterns or signatures in the mode 1 difference.

First, we note that there is a similarity between mean field differences and mode 1 component differences. It is clear that systematic changes contributing to the mean field changes occur according to El Niño mode, and they are indeed associated with the El-Niño-type changes over the last three decades. During the last decade (1999–2008), SSTs decreased; DC was suppressed; the upper troposphere became drier; and SLP became higher over the eastern tropical ocean than their corresponding values in the previous two decades (1978–1998). In contrast, the western Pacific revealed warmer SST, enhanced deep convective activities, a wetter upper troposphere, and slightly lower SLP during the last decade. Further, a strengthened east–west SLP gradient was established, causing strengthened easterlies. The stronger boundary-layer effective easterlies

over the central tropical Pacific are consistent with the strengthened east–west SLP gradient over the tropical Pacific (and thus strengthened Walker circulation).

The geographical distributions of SST changes are nearly the same as those in full-blown EP El Niño, except for the sign change, and the changes noted in other variables should be, in part, the atmospheric responses to the given SST changes. It is suggested that these structural changes reflected in the SST and other variables are likely due to fewer occurrences of EP El Niños during the last decade, as discussed in the EOF analysis. It is further suggested that the frequent occurrences of CP El Niños during the recent decades did not warm the eastern Pacific cold tongue as much as before, while still warming the western Pacific, resulting in a more La Niña-like pattern.

The EOF mode 1 (or El Niño mode) should have contributed to the basic mean field with a trend that reflects strengthened Walker circulation over the recent three decades. As more occurrences of the new type of CP El Niño in the recent decade brought about SST changes and changes in other variables consistent with the strengthened Walker circulation, we conclude that the decadal variations in El Niño cause the strengthened Walker circulation.

5 Changes in the Walker circulation in climate model simulations

Since there has been a strengthened Walker circulation for the last three decades caused by the shift of the El Niño pattern, it is of much interest to examine how climate models simulate increasing Walker circulation owing to the decadal variation in El Niño. Because the boundary-layer effective wind derived from water vapor transport mainly reflects the return flow from the subsidence region to the ascending region in the Walker circulation cell, we use the effective wind as an index of Walker circulation intensity. This analysis mainly focuses on the model outputs from the Program for Climate Model Diagnosis and Intercomparison (PCMDI), which participated in the Fourth Assessment Report (AR4) of the Intergovernmental Panel on Climate Change (IPCC). These archived data constitute phase 3 of the World Climate Research Programme (WCRP) Coupled Model Intercomparison Project (CMIP3; Meehl et al. 2007). Among 12 scenarios, the twentieth century climate (20C3M) and 720 ppm CO₂ stabilization experiment (SRESA1B) are used in this study. Outputs from a total of 21 model members are used for calculating boundary-layer effective winds. Available data vary for the 1850–2009 period; however, the datasets mainly cover the 1900–1999 period (twenty-first century, 100 years). Detailed descriptions about the models and datasets are found at http://www-pcmdi.llnl.gov/ipcc/about_ipcc.php.

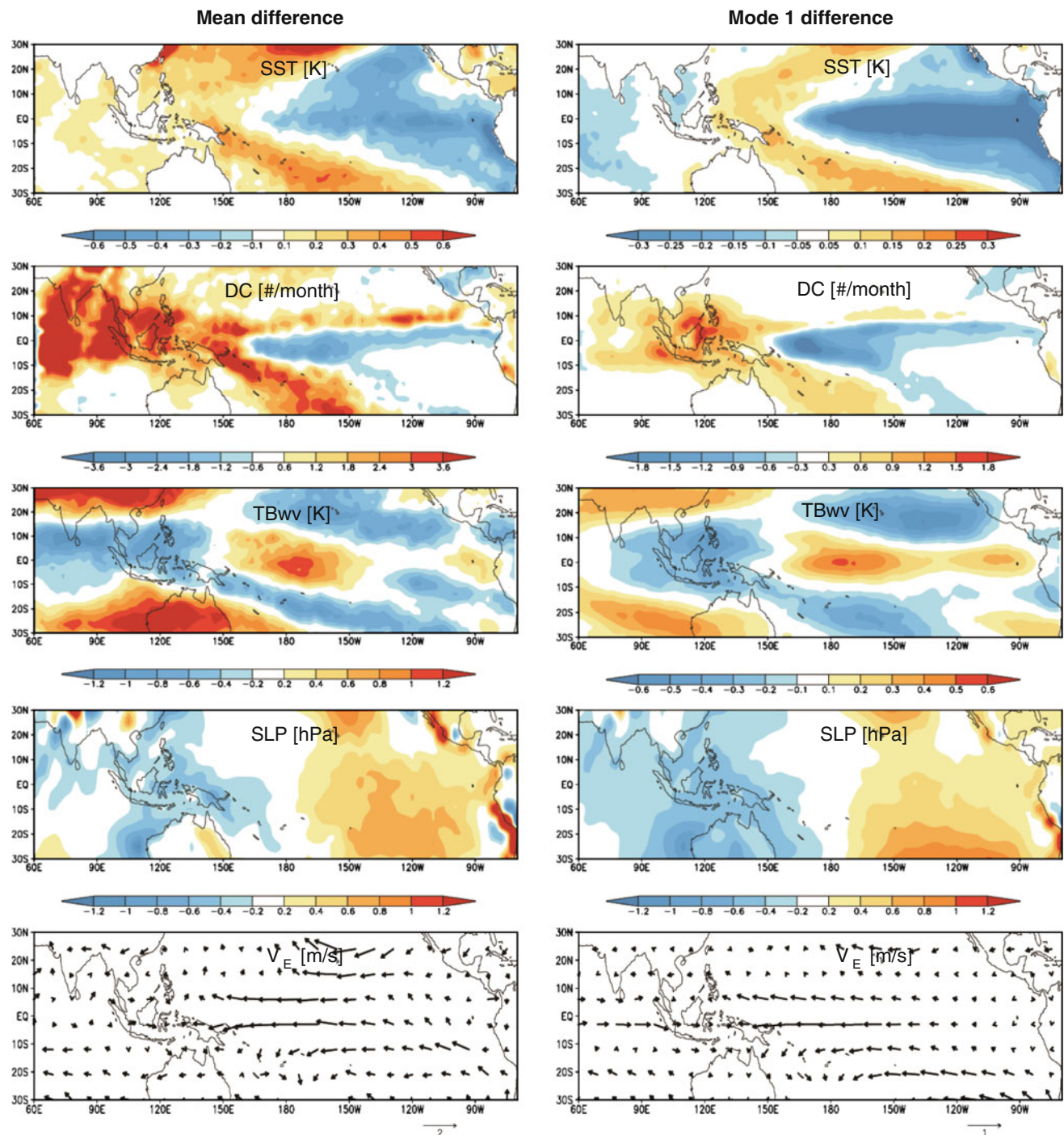


Fig. 3 Decadal differences (1999–2008 minus 1979–1998) of mean fields (*left panels*) and contributions to the mean fields by EOF mode 1 (*right panels*)

To examine the changes in Walker circulation, the east–west component of the boundary-layer effective wind is averaged over the tropical Pacific domain (120°E – 120°W , 12.5°N – 12.5°S), as in Sohn and Park (2010). However, in contrast to the index used by Sohn and Park (2010), the easterly wind is considered positive so that the increased effective easterly wind can be interpreted as an intensified

Walker circulation. The magnitude of the averaged easterly component of the boundary-layer effective wind over the chosen box is defined as a Walker circulation index (now referred to as WCI).

The WCI time series are given in Fig. 4a and associated trends for the data-available periods after 1979 are given in Fig. 4a. In this plot, three CGCM outputs (GFDL-CM2.0,

GFDL-CM2.1, and ECHAM5/MPI-OM) are highlighted since they are considered to be best models for simulating ENSO statistics (Van Oldenborgh and Burgers 2005). The corresponding WCI trends are calculated from times series, and results are given in Fig. 4b. The horizontal line in Fig. 4b represents a WCI trend of 0.062 m s^{-1} per 10 years, inferred from the SSM/I estimate of WCI (Fig. 5 of Sohn and Park 2010). Note that there seems to be no agreement regarding the weakening or strengthening of the Walker circulation amongst the 21 CMIP participating models; 11 models show strengthened Walker circulation at least over the 20 years from 1979, whereas 10 models show weakened Walker circulation. Moreover, WCI trends are much smaller than the SSM/I-suggested value of 0.062 m s^{-1} per 10 years, even if only results showing positive trends are considered (Fig. 4b). The fact that the range of GCM Walker circulation trends over the last 30 years is far different from the observed trend may indicate that there exist large uncertainties and biases in CMIP3 models in simulating the strengthened Walker circulation in recent decades. Because the twentieth century climate scenario run is driven by a realistic external forcing in the present climate, we expect the CMIP3 model outputs to be similar to the range of the observed atmospheric circulation (here, strengthened Walker circulation). However, the lack of consensus amongst model outputs strongly suggests that uncertainties in model outputs are too large to reproduce decadal variations in El Niño in terms of their spatial pattern and thus appear to be too uncertain to discuss the strengthened Walker circulation in recent decades using model outputs. According to recent study (Ham and Kug 2012), most of the CMIP3 models have serious systematic problems in simulating the distinctive SST patterns associated with the CP and EP El Niño. Therefore, we suspect that the failure to accurately simulate the two types of El Niño (i.e., CP and EP El Niño) in the CMIP3 models may have led to unsuccessful simulations of the strengthened Walker circulation observed in recent decades.

6 Summary and discussion

We considered the intensified Walker circulation in recent decades as a working hypothesis. Variations in meteorological or surface variables are expected to agree with the intensified circulation, i.e., increased deep convective activities and associated upper tropospheric moistening over the western Pacific ascending region and increased SLP over the eastern Pacific descending region in contrast to decreased SLP over the western Pacific ascending region; an enhanced easterly wind is expected in the boundary layer over the entire tropical Pacific basin in

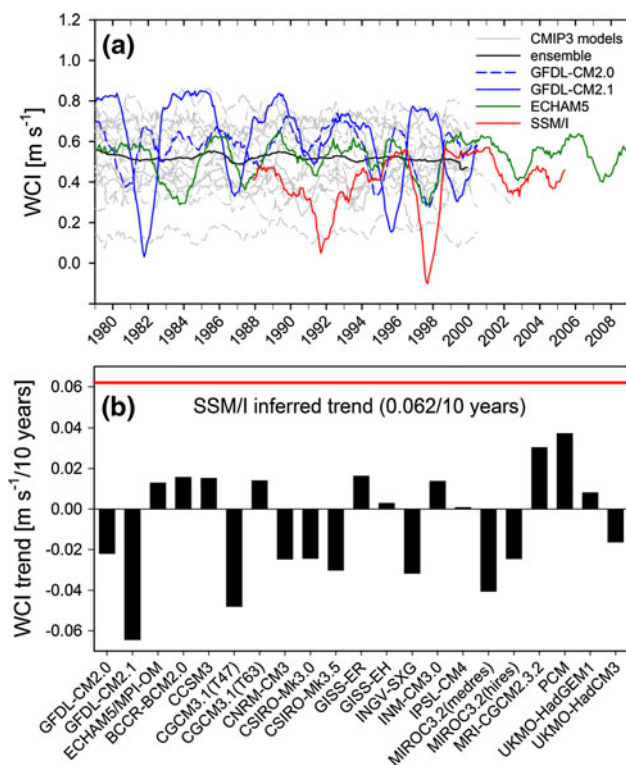


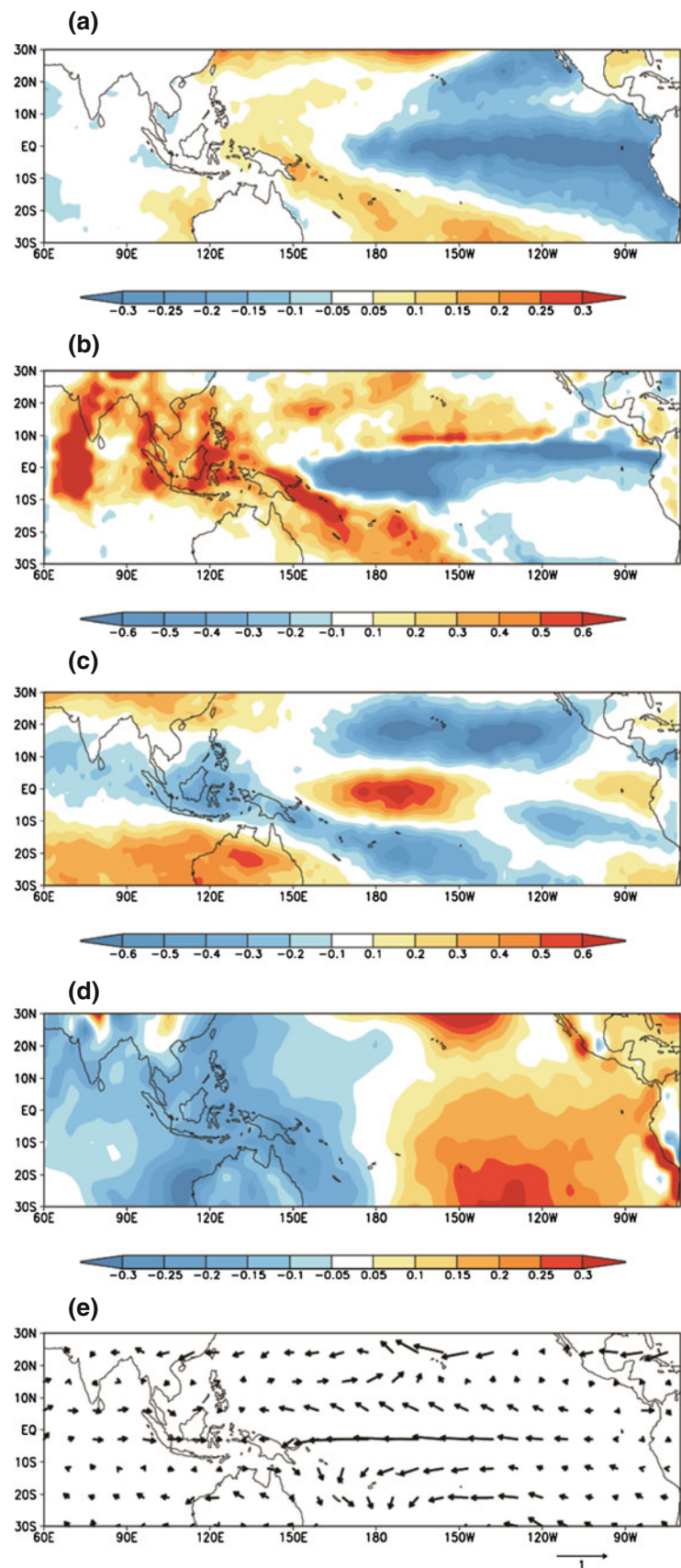
Fig. 4 **a** Time series of the Walker circulation index (WCI) for 21 CMIP3 model outputs and SSM/I. **b** WCI trend calculated for the available data period after 1979. In **b**, the red horizontal line represents the WCI trend inferred from the WCI time series for SSM/I in **a**. Definition of WCI is found in the text

response to the increased east–west SLP gradient. The results shown in this study are rather consistent with such expected changes in meteorological variables, indicating that the Walker circulation should have intensified over the past three decades.

As a cause of the intensified Walker circulation, we proposed the frequent occurrences of CP El Niño in the most recent decade, as a result of which the eastern tropical Pacific and western Pacific have undergone cooling and warming, respectively, over the three decades. All other variables (deep convective clouds, UTH, SLP, boundary-layer effective wind from the water vapor transport field) over the 1979–2008 period, whose datasets are independent of each other, clearly demonstrate that their variations and trends are coherent with the SST trend caused by the shift in the type of El Niño and are thus consistent with the intensified Walker circulation. As the signals produced by El Niño modes of variables closely resemble the mean field changes, it is further suggested that the decadal variation in El Niño should be the main contributor to the intensified Walker circulation.

The climate models appear to be unsuccessful in reproducing such trends. The uncertainties in the current climate models may be attributed to the natural variability

Fig. 5 The spatial pattern of regressed **a** SST, **b** DC, **c** TB_{wv} , **d** SLP, and **e** V_E against the PDO index for the period of 1979–2008



dominating the forced signal over the tropical Pacific during the last three decades in the twentieth century climate scenario runs by CMIP3 CGCMs or to the fact that the models are not accurate enough to produce the decadal oscillations that caused the strengthened east–west SST gradient. The 30-year analysis period, however, appears too short to discuss whether the strengthened Walker circulation is due to global warming or natural variation in the Earth-atmosphere climate system independent of the warming trend; Chadwick et al. (2012) described a GCM experiment where multi-decadal SST changes in the tropical Pacific cause the Walker circulation to oppose the anthropogenically-forced mean change in the tropical circulation for several decades.

Apart from these results, other mechanisms that could explain the increased Walker circulation exist. For example, the mean background state change over the three decades might be connected to the Interdecadal Pacific Oscillation (IPO; Parker et al. 2007) or Pacific Decadal Oscillation (PDO; Mantua et al. 1997), which is the most dominant SST variability in the Pacific Ocean on the low-frequency timescales. Examining the possible connection of the strengthened Walker circulation to the IOP or PDO, SST, DC, TB_{WV} , SLP, and V_E are regressed against the monthly PDO index (Mantua et al. 1997) over the analysis period (Fig. 5). Because the IPO index shows a negative trend since 1980, its regressed SST pattern is characterized by a triangular shape of cooler SST in the tropical eastern Pacific (i.e., La Niña-like condition) (Fig. 5a). The regressed patterns of DC, TB_{WV} , SLP, and V_E (Fig. 5b–e) all appear to be well correlated with the SST pattern, showing similar behaviors noted in the EOF analysis (Fig. 1). Therefore, one cannot rule out the PDO (IPO) in the Pacific Ocean basin on the low-frequency time scales as a possible cause of inducing the change of tropical Pacific mean state toward a more La Niña-like condition.

Conversely, one may argue that the intensified background Walker circulation can cause changes in El Niño characteristics. According to previous studies (Kug et al. 2009; Lee and McPhaden 2010; McPhaden 2012), it has been suggested that the mechanism of CP El Niño occurrence is closely associated with the zonal advective feedback process, in which anomalous zonal currents and mean SST zonal gradient are combined to enhance SSTs over the western Pacific. Thus, an enhanced Walker circulation may contribute to an increased zonal advective feedback by changing the mean SST zonal gradient and anomalous zonal currents through air–sea coupled processes in the tropical Pacific. In addition, it may be possible that the enhanced Walker circulation leads to a strong atmospheric stability over the eastern tropical Pacific due to the stronger sinking motion, which brings in weak ocean-atmospheric feedback processes there. Under such conditions the

occurrence of EP El Niño may be suppressed, changing El Niño characteristics. By taking all these possible connections between the increased Walker circulation and SST variations into account, much effort including model experiments would be needed to explore more details of these interactions.

Acknowledgments The authors would like to thank two anonymous reviewers for their constructive and valuable comments, which led to an improved paper. This work was supported by the National Research Foundation of Korea (NRF) Grant (NRF-2011-C00033).

Open Access This article is distributed under the terms of the Creative Commons Attribution License which permits any use, distribution, and reproduction in any medium, provided the original author(s) and the source are credited.

References

- Allan R, Ansell T (2006) A new globally complete monthly historical gridded mean sea level pressure dataset (HadSLP2): 1850–2004. *J Clim* 19:5816–5842
- Ashok K, Behera SK, Rao SA, Weng H, Yamagata T (2007) El Niño Modoki and its possible teleconnection. *J Geophys Res* 112:C11007. doi:10.1029/2006JC003798
- Cane MM, Clement AC, Kaplan A, Kushnir Y, Pozdnyakov D, Seager R, Zebiak SE, Murtugudde R (1997) Twentieth-century sea surface temperature trends. *Science* 275:957–960
- Chadwick R, Wu P, Good P, Andrews T (2012) Asymmetries in tropical rainfall and circulation patterns in idealised CO₂ removal experiments. *Clim Dyn*. doi:10.1007/s00382-012-1287-2
- Chung ES, Sohn BJ, Schmetz J (2009) Diurnal variation of outgoing longwave radiation associated with high cloud and UTH changes from Meteosat-5 measurements. *Meteorol Atmos Phys* 105:109–119. doi:10.1007/s00703-009-0041-8
- Clement AC, Seager R, Cane MA, Zebiak SE (1996) An ocean dynamical thermostat. *J Clim* 9:2190–2196
- Deser C, Phillips AS, Alexander MA (2010) Twentieth century tropical sea surface temperature trends revisited. *Geophys Res Lett* 37:L10701. doi:10.1029/2010GL043321
- Feng M, McPhaden MJ, Lee T (2010) Decadal variability of the Pacific subtropical cells and their influence on the southeast Indian Ocean. *Geophys Res Lett* 37:L09606. doi:10.1029/2010GL042796
- Ham Y-G, Kug J-S (2012) How well do current climate models simulate two types of El Niño? *Clim Dyn*. doi:10.1007/s00382-011-1157-3
- Held IM, Soden BJ (2006) Robust responses of the hydrological cycle to global warming. *J Clim* 19:5686–5699
- IPCC (2007) Climate change 2007: the physical science basis. Contribution of working group I to the fourth assessment report of the Intergovernmental Panel on Climate Change. Cambridge University Press, Cambridge
- Jakob C, Tselioudis G (2003) Objective identification of cloud regimes in the Tropical Western Pacific. *Geophys Res Lett* 30(21):2082. doi:10.1029/2003GL018367
- Kao H-Y, Yu J-Y (2009) Contrasting eastern-Pacific and central-Pacific types of ENSO. *J Clim* 22:615–632
- Karnauskas KB, Seager R, Kaplan A, Kushnir Y, Cane MA (2009) Observed strengthening of the zonal sea surface temperature gradient across the equatorial Pacific Ocean. *J Clim* 22:4316–4321

- Kug J-S, Jin F-F, An S-I (2009) Two types of El Niño events: cold tongue El Niño and warm pool El Niño. *J Clim* 22:1499–1515
- L'Heureux ML, Collins DC, Hu Z-Z (2012) Linear trends in sea surface temperature of the tropical Pacific Ocean and implications for the El Niño–Southern Oscillation. *Clim Dyn*. doi:10.1007/s00382-012-1331-2
- Larkin NK, Harrison DE (2005) On the definition of El Niño and associated seasonal average U.S. weather anomalies. *Geophys Res Lett* 32:L13705. doi:10.1029/2005GL022738
- Lee T, McPhaden MJ (2010) Increasing intensity of El Niño in the central-equatorial Pacific. *Geophys Res Lett* 37:L14603. doi:10.1029/2010GL044007
- Levitus S, Antonov JI, Boyer TP, Locarnini RA, Garcia HE, Mishonov AV (2009) Global ocean heat content 1955–2008 in light of recently revealed instrumentation problems. *Geophys Res Lett* 36:L07608. doi:10.1029/2008GL037155
- Mantuna NJ, Hare SR, Zhang Y, Wallace JM, Francis RC (1997) A Pacific interdecadal climate oscillation with impacts on salmon production. *Bull Am Meteorol Soc* 78:1069–1079
- McPhaden MJ (2012) A 21st century shift in the relationship between ENSO SST and warm water volume anomalies. *Geophys Res Lett* 39:L09706. doi:10.1029/2012GL051826
- McPhaden MJ, Lee T, McClurg D (2011) El Niño and its relationship to changing background conditions in the tropical Pacific Ocean. *Geophys Res Lett* 38:L15709. doi:10.1029/2011GL048275
- Meehl GA, Covey C, Delworth T, Latif M, McAvaney B, Mitchell JFB, Stouffer RJ, Taylor KE (2007) The WCRP CMIP3 multimodel dataset: a new era in climate change research. *Bull Am Meteorol Soc* 88:1383–1394
- Meng Q, Latif M, Park W, Keenlyside NS, Semenov VA, Martin T (2011) Twentieth century Walker circulation change: data analysis and model experiments. *Clim Dyn*. doi:10.1007/s00382-011-1047-8
- Merrifield MA (2011) A shift in western tropical Pacific sea level trends during the 1990s. *J Clim* 24:4126–4138
- O'Carroll AG, Saunders RW, Watts JG (2006) The measurement of the sea surface temperature by satellites from 1991 to 2005. *J Atmos Ocean Technol* 23:1573–1582
- Park J-Y, Yeh S-W, Kug J-S (2012) Revisited relationship between tropical and North Pacific Sea surface temperature variations. *Geophys Res Lett* 39:L02703. doi:10.1029/2011GL050005
- Parker D, Folland C, Scaife A, Knight J, Colman A, Baines P, Dong B (2007) Decadal to multidecadal variability and the climate change background. *J Geophys Res* 112:D18115. doi:10.1029/2007JD008411
- Philander SG (1989) *El Niño, La Niña, and the Southern Oscillation*. Academic Press, London
- Rayner NA, Parker DE, Horton EB, Folland CK, Alexander LV, Rowell DP, Kent EC, Kaplan A (2003) Global analyses of sea surface temperature, sea ice, and night marine air temperature since the late nineteenth century. *J Geophys Res* 108:4407. doi:10.1029/2002JD002670
- Roca R, Guzman R, Lemond J, Meijer J, Picon L, Brogniez H (2012) Tropical and extra-tropical influences on the distribution of free tropospheric humidity over the intertropical belt. *Surv Geophys*. doi:10.1007/s10712-011-9169-4
- Rosow WB, Tselioudis G, Polak A, Jakob C (2005) Tropical climate described as a distribution of weather states indicated by distinct mesoscale cloud property mixtures. *Geophys Res Lett* 32:L21812. doi:10.1029/2005GL024584
- Seager R, Murtugudde R (1997) Ocean dynamics, thermocline adjustment, and regulation of tropical SST. *J Clim* 10:521–534
- Shi L, Bates JJ (2011) Three decades of intersatellite-calibrated High-Resolution Infrared Radiation Sounder upper tropospheric water vapor. *J Geophys Res* 116:D04108. doi:10.1029/2010JD014847
- Simmons A, Uppala S, Dee D, Kobayashi S (2006) ERA-Interim: new ECMWF reanalysis products from 1989 onwards. *ECMWF Newsl* 110:25–35
- Smith TM, Reynolds RW, Peterson TC, Lawrimore J (2008) Improvements to NOAA's historical merged land-ocean surface temperature analysis (1880–2006). *J Clim* 21(10):2283–2296
- Soden BJ, Bretherton FP (1993) Upper tropospheric relative humidity from the GOES 6.7 μm channel: method and climatology for July 1987. *J Geophys Res* 98(D9):16669–16688. doi:10.1029/93JD01283
- Sohn B-J, Park S-C (2010) Strengthened tropical circulations in past three decades inferred from water vapor transport. *J Geophys Res* 115:D15112. doi:10.1029/2009JD013713
- Sohn B-J, Smith EA, Robertson FR, Park S-C (2004) Derived over-ocean water vapor transports from satellite-retrieved E-P datasets. *J Clim* 17:1352–1365
- Sohn B-J, Schmetz J, Chung E-S (2008) Moistening processes in the tropical upper troposphere observed from Meteosat measurements. *J Geophys Res* 113:D13109. doi:10.1029/2007JD009527
- Sun D-Z, Liu Z (1996) Dynamic ocean–atmosphere coupling, a thermostat for the tropics. *Science* 272:1148–1150
- Tselioudis G, Tromeur E, Rosow WB, Zerefos CS (2010) Decadal changes in tropical convection suggest effects on stratospheric water vapor. *Geophys Res Lett* 37:L14806. doi:10.1029/2010GL044092
- Van Oldenborgh GJ, Burgers G (2005) Searching for decadal variations in ENSO precipitation teleconnections. *Geophys Res Lett* 32:L15701. doi:10.1029/2005GL023110
- Vecchi GA, Soden BJ (2007) Global warming and the weakening of the tropical circulation. *J Clim* 20:4316–4340
- Vecchi GA, Clement A, Soden BJ (2008) Pacific signature of global warming: El Niño and La Niña? *EOS Trans Am Geophys Union* 89(9):81–83
- Yeh S-W, Kug J-S, Dewitte B, Kwon M-H, Kirtman B, Jin F-F (2009) El Niño in a changing climate. *Nature* 461:511–514
- Zahn M, Allan RP (2011) Changes in water vapor transports of the ascending branch of the tropical circulation. *J Geophys Res* 116:D18111. doi:10.1029/2011JD016206
- Zhou YP, Xu K-M, Sud YC, Betts AK (2011) Recent trends of the tropical hydrological cycle inferred from Global Precipitation Climatology Project and International Satellite Cloud Climatology Project data. *J Geophys Res* 116:D09101. doi:10.1029/2010JD015197